Chapter 1

Introduction

This chapter highlights the historical development of Raman spectroscopy and its principles and instrumentation. The mechanism of surface enhanced Raman scattering (SERS) has been thoroughly discussed. Evolution of SERS substrate and parameters that determine/control the enhancement factor of SERS substrate are also discussed. In the last part of this chapter, the objective and scope of the thesis work have been discussed.

1.1 A brief overview of Raman scattering

Raman scattering is an inelastic light scattering process from the molecules/compounds whose size is comparable to the wavelength of incident monochromatic light. Inelastic scattering is nothing but shifting of frequency in the scattered light from the incident light. Raman spectroscopy, being a vibrational spectroscopic technique has emerged as a convincing and reliable technique for label-free detection and identification of a specific molecule in unknown samples. This specific spectroscopic technique is used in wide range of fields that includes explosives detection, bacteria identification, living cell analysis, DNA and RNA detection, protein-protein interaction and analysis etc.[1-7]. Raman spectroscopy has several advantages such as no or very few sample preparation steps are required, in-situ and in-vitro investigations for biological samples is possible, non-destructive and non-invasive investigations of samples are possible with this technique [8-10]. Also, samples can be examined either in solid, liquid or vapor phase, in hot or cold environment, in bulk or microscopic particles, or as surface layers.

1.1.1 The discovery of Raman effect

The inelastic scattering of light was first postulated by Smekal in 1923 [11] and later in 1928 Raman and Krishnan [12] confirmed this phenomenon experimentally. Then onward this specific phenomenon is termed as Raman scattering and applications of this phenomenon in different fields of study is called, as Raman spectroscopy. In the first experimental demonstration of this process, violet spectrum from sunlight was allowed to pass through a liquid droplet. They observed that same color light had emerged from the liquid sample. However, by placing a green filter between observer and sample they could see light of different color than that of the incident color. From this experimental observation, they reported that a part of scattered light has different frequencies than the incident frequency. In the first Raman spectrometer, sunlight was focused onto the sample through a telescope and another lens was placed to collect the scattered radiation. To make the Raman analysis more accurate rather than the visual and qualitative observation, Raman replaced the observer by quartz spectrograph with which he could photograph the spectrum of the scattered light and measure its wavelength shift due to inelastic scattering of light from the sample.

1.1.2 Theory of Raman scattering

The phenomenon of Raman scattering can be described in two ways, the classical wave interpretation and the quantum particle interpretation. Light is considered as electromagnetic radiation in the classical wave interpretation. It contains an oscillating electric field and interacts with a molecule through its polarizability. The polarizability of a molecule is nothing but the ability to interact with an electric field which is determined by the electron clouds. On the other hand, in case of quantum particle interpretation, light is considered as a group of photons that strikes the molecule and then scattered inelastically. The number of scattered photons depends on the molecular structure and environment, such as atomic mass, bond order, molecular constituents, molecular geometry etc. Figure 1.1 shows a visual comparison of these two methods.

To derive classical interpretation of Raman mathematically, consider a diatomic molecule as a mass on a spring as shown in figure 1.2. Where m represents the atomic mass, x represents the displacement, and K represents the bond strength. Using Hooke's

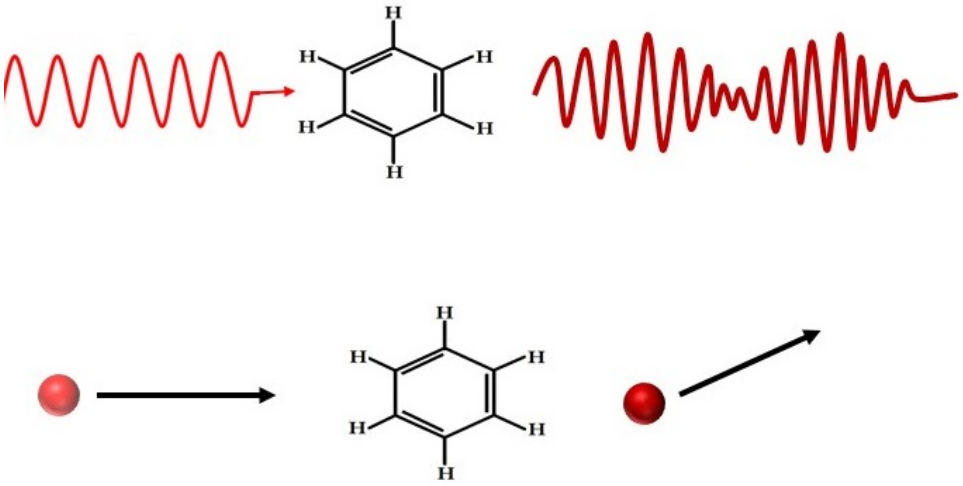

Figure 1.1: Classical wave and quantum particle interpretation of Raman scattering

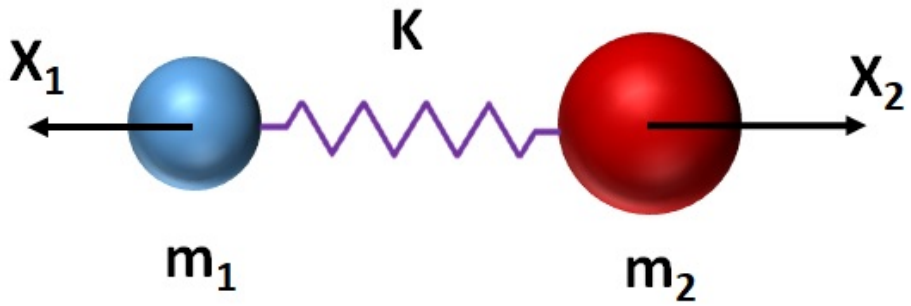

Figure 1.2: Diatomic molecule as amass on spring

law, the displacement of the molecule can be obtained as,

$$\frac{m_1 \times m_2}{m_1 + m_2}\left(\frac{d^2x_1}{dt^2} + \frac{d^2x_2}{dt^2}\right) = -K(x_1 + x_2) \tag{1.1}$$

Replacing the reduced mass $\frac{m_1 \times m_2}{m_1 + m_2}$ and the total displacement $x_1 + x_2$ with μ and q respectively, the equation can be obtained as,

$$\mu(\frac{d^2q}{dt^2}) = -Kq \tag{1.2}$$

Solving this equation for q we have,

$$q = q_0 cos(2\pi\nu_m t) \tag{1.3}$$

where q_0 is the amplitude of the molecular vibration and v_m is the frequency of the

molecular vibration and is defined as,

$$v_m = \frac{1}{2\pi}\sqrt{\frac{K}{\mu}} \tag{1.4}$$

From equations 1.3 and 1.4, it is seen that the molecular vibration is sinusoidal in nature and the frequency of the vibration is proportional to the bond strength and inversely proportional to the reduced mass. This ensures that each and every molecule will have their unique vibrational signatures, which are determined not only by the atoms in the molecule, but also the characteristics of the individual bonds [13]. When electromagnetic (EM) radiation is incident on the material, the electric field associated with the EM radiation induces an electric dipole moment M in the molecule and is given by

$$M = \alpha E \tag{1.5}$$

where α is the polarizability of the molecule. The electric field E is given by

$$E = E_0 cos(\omega t) = E_0 cos(2\pi\nu t) \tag{1.6}$$

where E_0 is the amplitude and ν is the frequency of the incident electric field.
From equations 1.5 and 1.6, M can be obtained as,

$$M = \alpha E_0 cos(2\pi\nu t) \tag{1.7}$$

The dipole is oscillating in nature and oscillating dipole emits radiation at its own oscillating frequency ν, giving the Rayleigh scattered beam. However, the polarizability varies slightly with molecular vibration and is given by

$$\alpha = \alpha_0 + q\left(\frac{d\alpha}{dq}\right)_{q=0} + ... \tag{1.8}$$

here, q describes the molecular vibration as obtained in equation 1.3. From equations 1.3 & 1.8, we have

$$\alpha = \alpha_0 + q_0\left(\frac{d\alpha}{dq}\right)_{q=0} cos(2\pi\nu_m t) \tag{1.9}$$

Substituting for α in equation 1.7, we have

$$M = \alpha_0 E_0 cos(2\pi\nu t) + q_0 cos(2\pi\nu_m t) E_0 cos(2\pi\nu t)\left(\frac{d\alpha}{dq}\right)_{q=0} \tag{1.10}$$

Using the trigonometric identity, $cosA + cosB = \frac{1}{2}(cos(A+B) + cos(A-B))$ equation

1.10 can be rewritten as-

$$M = \alpha_0 E_0 cos(2\pi\nu t) + \frac{1}{2} q_0 E_0 \left(\frac{d\alpha}{dq}\right)_{q=0} (cos(2\pi(\nu + \nu_m)t) + (cos(2\pi(\nu - \nu_m)t)) \quad (1.11)$$

Thus, we find that the oscillating dipole has three distinct frequency components- The exciting frequency ν, with amplitude $\alpha_0 E_0$, and shifting frequency $\nu+\nu_m$ and $\nu-\nu_m$ with very small amplitude of $\frac{1}{2} q_0 E_0 \left(\frac{d\alpha}{dq}\right)_{q=0}$. From equation 1.11, it is observed that due to the interaction of light with the molecule, there could be two resultant effects. The first effect is called Rayleigh scattering, which is the dominant part of the scattering process and results, no change in the frequency of the scattered light. The second one is the Raman scattering effect, where the frequency of the scattered light is shifted by plus or minus of the molecular vibration frequency of the molecule. The increase in frequency is known as an anti-Stokes shift and the decrease in frequency is known as a Stokes shift. Thus, Raman spectrum in principle directly provides the vibrational frequency of a molecular bond. If the molecular vibration does not change, the polarizability of the molecule would be then $\frac{1}{2} q_0 E_0 \left(\frac{d\alpha}{dq}\right)_{q=0} = 0$. In this case, the dipole oscillates only at the frequency of the incident (exciting) radiation. Thus, to have Raman spectrum of the molecule, the molecular vibration or rotation must cause a change in the molecular polarizability. The classical interpretation of Raman effect satisfactorily describes the

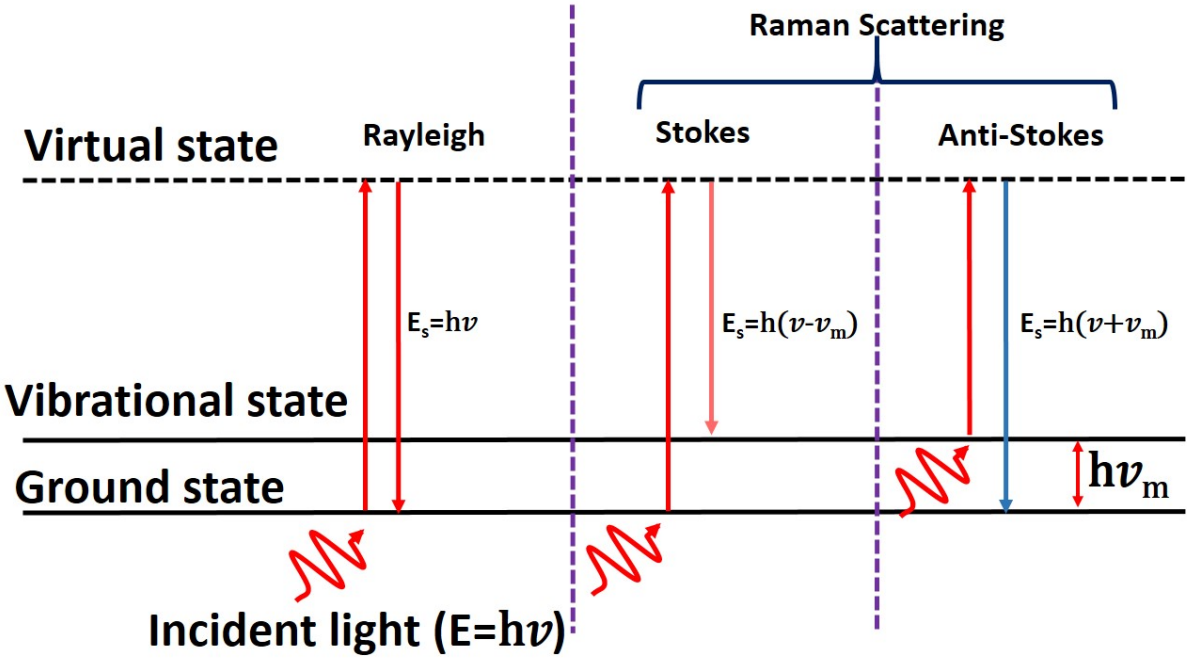

Figure 1.3: Energy level diagram for Rayleigh scattering, Stokes Raman scattering and anti-Stokes Raman scattering

Rayleigh scattering, Stokes and anti-Stokes shift with their frequency and amplitudes.

The intensities of anti-Stokes lines are much weaker than Stokes lines. The reason behind this anomaly cannot be explained by the classical interpretation, therefore the quantum particle interpretation came into picture. To have, better visualization of the Raman effect and to determine additional information, the quantum particle interpretation can be used. The Raman effect is described as an inelastic scattering of a photon from a molecule. From figure 1.3, it is seen that the incident photon exciting the molecule into a virtual energy state. There are three different potential outcomes when it occurs. First, the molecule can bounce back to the ground state by emitting a photon of equal energy to that of the incident photon, which is referred as Rayleigh scattering. Secondly, the molecule can relax to a higher vibrational state by emitting a photon with less energy than the incident photon, this is called Stokes shifted Raman scattering. The third potential outcome is that the molecule already exist in the excited vibrational state is excited to a higher virtual state and then return to the ground state by emitting a photon with more energy than the incident photon, this is called anti-stokes Raman scattering. At room temperature the population of molecules in the ground state in general is more than higher vibrational state, therefore probability that a scattered photon will be anti-Stokes is much lower than Stokes line, hence, scattering intensity of anti-Stokes shifted Raman signal is lower than the Stokes Raman scattering intensity. As a result, most Raman measurements are performed considering only the Stokes shifted light. Further, it has been observed that the power of the scattered light, P_S, is equal to the product of the intensity of the incident photons, I_0, and value known as the Raman cross-section, α_R. The Raman cross section is given by

$$\sigma_R \propto \frac{1}{\lambda^4} \tag{1.12}$$

where λ equals the wavelength of the incident photon. Therefore,

$$P_s \propto \frac{I_0}{\lambda^4} \tag{1.13}$$

From equation 1.13 it is seen that the power of the scattered light is directly proportional to the intensity of the incident light and inversely proportional to fourth power wavelength. Therefore, it is always desirable to use a short excitation wavelength and a high power excitation source based on these relationships. However, this is not always the case, because high power laser may some times burn the sample which will lead to loss of Raman spectra of the sample.

1.1.3 Raman instrumentation

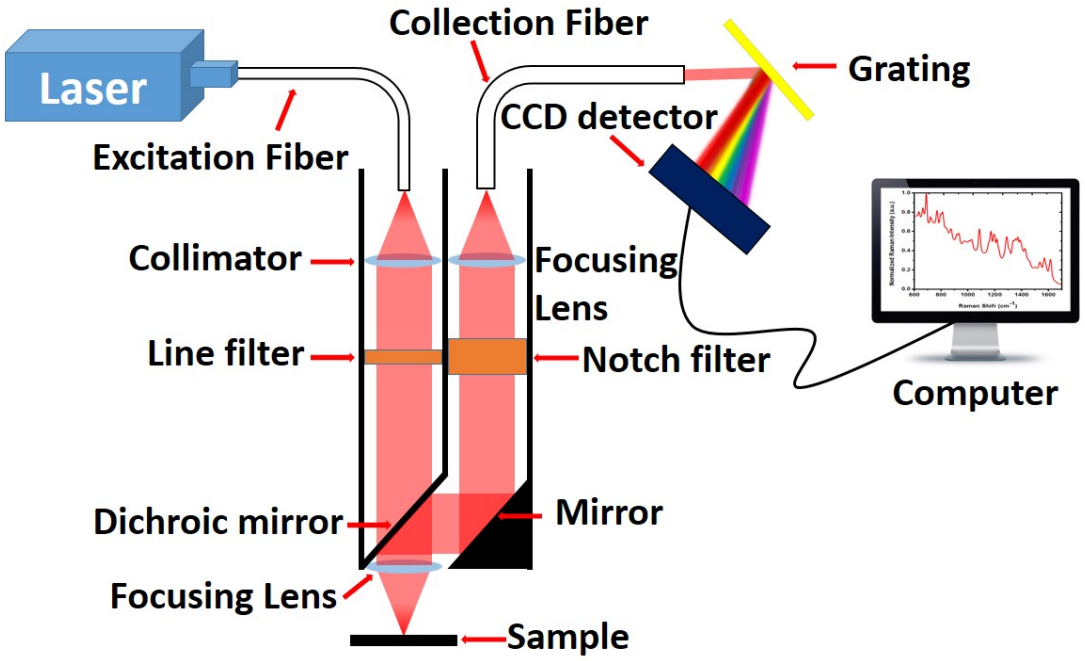

Figure 1.4: Schematic of a Raman spectrometer

The components used in the Raman spectrometer has been evolved over the years. All Raman spectrometers have three primary components namely an excitation source, sampling apparatus, and detector. In modern Raman spectrometer laser is used as excitation source, optical fiber and/or microscope as sampling apparatus and the spectrometer is used for detection and analysis of scattered Raman signal from the sample. Figure 1.4 shows the schematic of modern Raman spectrometer. The modern Raman system contains following main components- (a) a laser source, (b) excitation delivery optics, (c) sample, (d) collection optics, (e) a wavelength separation device, (f) detector and associated electronics and (g) a recording device. As Raman analysis is based on shift in wavelength, it is necessary to employ monochromatic light source for excitation. Laser with an extremely stable frequency typically is the best choice for use as an excitation source. It is also essential to utilize a clean, narrow bandwidth laser source, because the quality of Raman peaks is dependent on the sharpness and stability of the excitation light source. The intensity of Raman scattering is proportional to the fourth power of the excitation laser frequency, therefore short-wavelength laser sources yield intense Raman signal intensity. But higher fluorescence emission and photodecomposition of sample greatly affect in this case. In order to minimize higher fluorescence emission and photodecomposition, near infrared (NIR) laser sources such as diode laser and Nd/YAG lasers are used in modern Raman spectrometers. A narrow band-pass filter is used between the

laser and the sample, which allows a single laser line. The back scattered signal from the sample to the detector has to pass through a notch filter before being incident on the detector. The notch filter rejects 99.5% laser line and allows more than 90% other frequency lines. As Raman scattering is very weak therefore it is necessary to use a highly sensitive detector. Charge coupled devices (CCD) based detectors are commonly used in modern Raman spectrometer.

1.1.4 Limitation of Raman spectroscopy

Though Raman spectroscopy is a popular technique in recording the fingerprint of molecules, which are useful in the field of chemical science, biological science, environmental science and physical science, its wide range of applications is however limited. It is because out of 10^7 incident photon only 1 photon gets scattered inelastically and low order scattering cross section $\sim 10^{-30}$ cm^{-2}. Therefore, the intensity of Raman spectra of a Raman active molecule may not be in the range of measurable count. This specific limitation of Raman scattering has been overcome with the advent of surface enhanced Raman spectroscopy (SERS) which is a process mainly driven by localized surface plasmon resonance (LSPR) of metal nanostructures upon incident of EM field.

1.2 Surface enhanced Raman scattering (SERS) and its discovery

SERS is a phenomenon in which the Raman signal intensity of molecule is greatly enhanced when the molecule is absorbed or placed in close proximity to the metal nanostructure surface. This phenomenon was first observed in the year 1974, by Fleischmann and co-workers [14]. In their experiment, they observed intense Raman signals of pyridine when absorbed onto an electrochemically roughened silver surface. In their original paper, they interpreted that the amplified Raman signal of pyridine was due to increased surface area caused by the roughening of silver electrodes. Approximately three years later in 1977, two independent groups, Jeanmarie and R Van Duyne [15] and Albrecht and A Creighton [16] confirmed the result, in which they have observed Raman signal enhancement of about a million when compared with the signal from the pyridine molecules in the absence of metal. They documented that the observed Raman enhancement was not only due to increased surface area, instead, other mechanisms also contributed to the

enhancement. In the reported work, they proposed that the enhancement was due to LSPR condition of the metal nanopattern which would cause strong scattering of Raman signal. Several enhancement mechanisms were proposed by different researchers since the advent of SERS, however only two mechanisms namely Electromagnetic (EM) mechanism and Chemical Enhancement (CE) mechanism are now broadly accepted. The EM mechanism contributes dominantly (can contribute ten or more orders of magnitude) in the enhancement mechanism which is based on the collective oscillation of free electron density generating localized surface plasmons (LSPs) [17]. The CE mechanism describes the chemical interaction between probe molecules and the noble metal and is contribute only up to 2-3 orders of magnitude [18]. The principles of the above two enhancement mechanisms are discussed below.

1.2.1 Electromagnetic enhancement

It is important to recall the phenomenological approach to Raman scattering to understand the EM enhancement mechanism. When monochromatic radiation of frequency ν with an electric field E interacts with a molecule, it induces a dipole, oscillating at a frequency ν_m. The dipole moment is given by

$$M = \alpha E \tag{1.14}$$

The oscillating dipole radiates power proportional to M at frequency ν_m and the frequency detected as Raman signal in far-field. The same concept can be used to describe SERS. However, the roughened metal surface alters the effects as [19]
(a) There is a local field enhancement as a result of electromagnetic field enhancement at the metallic surface.
(b) The properties of radiation of the dipole are affected by the metallic environment resulting in possible radiation enhancement.

Local field enhancement: The electromagnetic field in the vicinity of metallic surfaces gets strongly modified upon incident of electromagnetic radiation on a suitable metal surface (that possess a negative real and small positive imaginary dielectric constant). This specific modification in the electromagnetic field is due to the coherent oscillation of free electrons that generate surface plasmons. Surface plasmons can be of two types, surface plasmon polariton (or propagating plasmon) that propagates along the metal-dielectric interface [20, 21] and localized surface plasmon which is localized on

the surface of a nanoparticle (figure 1.5) with a frequency known as the localized surface plasmon resonance (LSPR) [22, 23]. The local electric field E_L is different from incident

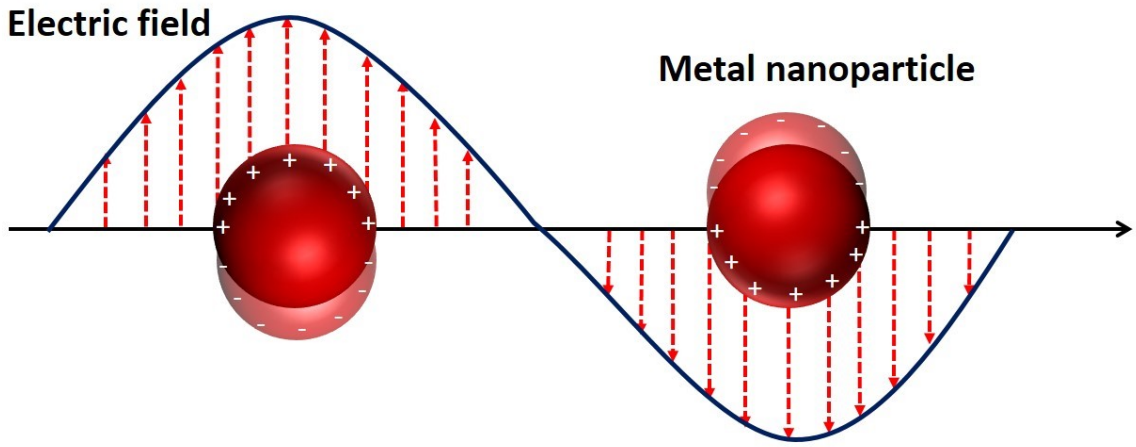

Figure 1.5: Schematic diagram of generation of localize surface plasmon

field E, in terms of both magnitude and orientation. Generally, the magnitude of $|E_L|$ can be much larger than $|E|$. The local field induces a dipole moment which is given by-

$$M_R = \alpha E_L \nu_m \tag{1.15}$$

Therefore, the dipole moment is enhanced by a factor of $\frac{|E_L \nu_m|}{|E|}$ as compared to the dipole induced due to incident field. If such dipole radiates in free-space (i.e., in absence of metallic environment), the radiated energy which is proportional to $|M_R|^2$, would be enhanced by a factor

$$EF_L = \frac{|E_L \nu_m|^2}{|E|^2} \tag{1.16}$$

The local electric field enhancement factor EF_L characterizes the enhancement of the electric field intensity. Here, orientation state of the electric field polarization has been ignored.

Radiation enhancement: In case of SERS conditions, the dipole moment induced due to the local field, radiates in close proximity to the metal and the metal strongly affects the dipole radiation. Depending on the relative dielectric function $\epsilon(r)$ of the metal, its geometry and the dipole position, orientation and its emission frequency (ν_{rad}), the total power radiated by the dipole (P_{rad}) can either increase or decrease (relative to that in free space, P_0). Due to the coupling of LSPR of metallic objects [24], there is

an enhancement in the radiated power. Therefore, the radiation enhancement factor is given by-

$$EF_{rad} = \frac{P_{rad}}{P_0} \tag{1.17}$$

$|E|^4$*Approximation:* Combining local electric field enhancement and radiation enhancement, EM enhancements of single-molecule SERS (SMSERS) can be expressed as [24]

$$EnhancementFactor(EF) \approx EF_L(\nu_m) \times EF_{rad}(\nu_{rad}) \tag{1.18}$$

By solving the electromagnetic problem under specific external excitation conditions with an incident field E, $EF_L(\nu_m)$ can be calculated. However, to estimate $EF_{rad}(\nu_{rad})$, one has to solve the electromagnetic problem of dipolar emission, instead of external excitation, which is a very complicated task. To avoid these complications, it is often assumed that local electric field enhancements and radiation enhancements are approximately equal. Hence, SERS enhancement factors can be expressed as

$$EF \approx EF_L(\nu_m) \times EF_{rad}(\nu_{rad}) \approx \frac{|E_L(\nu_m)|^2}{|E|^2}\frac{|E_L(\nu_R)|^2}{|E|^2} \tag{1.19}$$

An additional approximation can be made, i.e. $\nu_m = \nu_R$, which, results in famous expression of the SERS enhancement

$$EF \approx \frac{|E_L(\nu_m)|^4}{|E|^4} \tag{1.20}$$

1.2.2 Chemical enhancement

Different researchers have given many explanations to chemical enhancement mechanisms but the most accepted explanation of CE is the charge-transfer (CT) mechanism [24, 25] Due to adsorption of analyte on the metal surface, metal adsorbate complex is formed. There is a formation of covalent bond between adsorbate and metal surface (chemisorption). This bonding produces new electronic states and serves as resonant intermediate states. In other words, with the Fermi level of the metal, the highest occupied molecular orbital (HOMO) and the lowest unoccupied molecular orbital (LUMO) of the adsorbate are symmetrically disposed and charge transfers from Fermi level to LUMO and retrodonation of electron from HOMO to Fermi level of the metal as shown in the figure 1.6. Under this condition, transfer of charge from metal to molecule or vice versa can occur at an excitation energy equal to about half the energy required for intrinsic intramolec-

ular excitations of the adsorbate. Due to this mechanism, the analyte molecules that have their lowest-lying electronic excitations in the ultraviolet or near ultraviolet region is now shifted to visible region which eventually enables the SERS study of the analyte molecules.

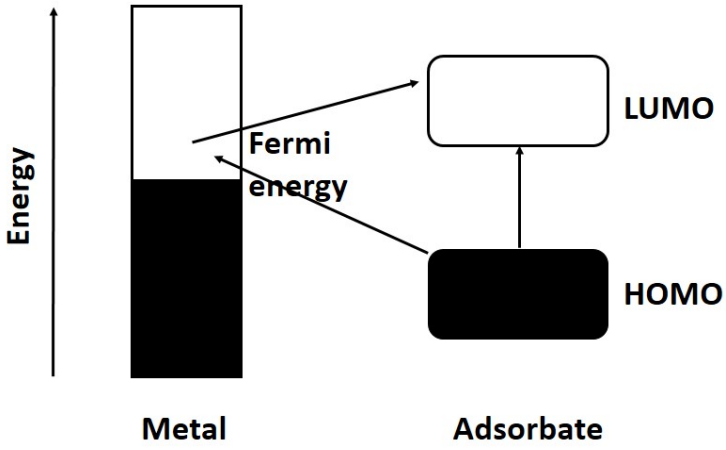

Figure 1.6: Schematic diagram of charge transfer mechanism

1.3 Enhancement factor

The enhancement factor (EF) is the key parameter to measure the performance of SERS substrate. It is the enhancement in the SERS signal intensity compared to normal Raman signal intensity of the same molecule under the same investigation environment. Depending on the application and nature of SERS substrates, the EF is evaluated in different ways. For simplicity, researchers evaluate analytical enhancement factor (AEF) using the following equation.

$$AEF = \frac{I_{SERS} \times C_R}{I_R \times C_{SERS}} \tag{1.21}$$

where I_{SERS} and I_R are SERS and Raman signal intensity of analyte molecule respectively. C_{SERS} and C_R are concentrations of same analyte used to measure SERS and Raman signal intensity. In this equation, it is assumed that both I_{SERS} and I_R linearly varies with incident power density and analyte concentrations. However, I_{SERS} implies

the scattered Raman signal intensity for surface absorbed analyte molecules only. Therefore, to calculate the EF of SERS substrate following equation is widely used by the researchers.

$$EF = \frac{I_{SERS} \times N_{REF}}{I_{REF} \times N_{SERS}} \tag{1.22}$$

where I_{SERS} is the SERS signal intensity, I_{REF} is the reference Raman signal intensity, N_{REF} and N_{SERS} are the number of molecules within the excitation volume on the reference substrate and on the sensing region of the SERS substrate respectively. The number of molecules within the excitation volume is calculated by using the relation $N = VcN_A$ where, V is the volume of the analyte excited by laser spot, c is the concentration of analyte and N_A is the Avogadro's number. This expression has been extensively used in evaluating the average EF [24, 26-28] of a SERS substrate. Some parameters such as wavelength, incident angle, polarization, substrate orientation with excitation source etc. also influence the SERS EF. Substrate fabrication parameters such as material, shape and size of the structures, nature of the substrate also suborned the SERS EF. Adsorption properties of analyte on the substrate and surface coverage also affect in SERS EF. For instance, for metal nanosphere [29-36] size, spacing between dimmers and periodicity; for nanotriangle and nanoprism [37, 38] metal thickness, edge length and corner truncation and roundness; for nanovoid [39-41] metal thickness and diameter to depth ratio; and for nanowire and nanorod [42-52] alignment, diameters, length and gap influence the SERS enhancement.

1.4 SERS substrate

The metal nanostructures platform that supports strong plasmon resonance can enhance weak Raman signals from the trapped analyte. SERS enhancement is typically due to resonance plasmon response of the substrates, that strongly depends on wavelength. A SERS substrate will exhibit good enhancement upon excitation with a proper wavelength source. Generally SERS substrates are designed to operate between 400-1000 nm excitation wavelength. While considering to design a SERS substrate it should necessarily (a) provide higher order of enhancement, (b) have larger surface area, (c) highly reproducible, (d) higher scattering volume and (e) easy to develop (not always applicable). Depending on the requirements and applications, different approaches have been adopted for development of SERS substrate. The SERS substrates can be broadly classified into three sub-categories-

1. Roughen metal electrode

2. Metal nanopartilce colloid
3. Metallic nanostructure array on planer substrates

1.5 Different approaches to develop SERS substrate

A large number of techniques have been adopted for the development of SERS substrate. To design SERS substrate, basically wet chemical bottom-up method and top-down lithographic techniques are used. In early stage of this field, roughened metallic electrodes were used as SERS substrate. The roughen electrodes were generally obtained through oxidation and reduction cycles in electrochemical cell. These methods generate non-uniform substrate with roughening feature size of 25-500 nm [53]. This kind of substrates are relatively easy to generate but it suffers low SERS enhancement. With the advancement of etching technique substrate with uniform and controlled roughness with feature size as small as 100 nm is achievable [54]. Due to its simplicity and low-cost approach, this technique is still an active area of interest [55]. Metallic nanoparticle colloidal solution is extensively used as SERS substrate as it is easy to design and produce higher order SERS enhancement [56]. Detection of single molecule has also been demonstrated with such substrate [57]. Spherical nanoparticle colloids mostly of Au or Ag are the first and most widely used colloidal SERS substrate. Other complex shapes such as nano prism, nanorods, nanostars, nanotriangles, nanocubes etc. [53] fabricated using seed mediated growth technique have been used for different SERS based studies. More complex structures- branched metal Nanoflowers [58], polyhedral nanocrystals [59] and capped dendritic Au NPs [60] have also been fabricated. However, these kinds of substrates yields poor reproducibility due to random distribution of nanoparticle aggregation. By immobilizing the metal nanoparticles on solid surface the poor reproducibility of metal nanoparticle colloids can be reduced. Generally, chemical functionalization or self-assemble techniques are used to attach metal nanoparticles [61] on the substrate.

The reproducibility of SERS substrate can be improved by fabricating ordered array of nanostructures on plane substrate. Techniques such as electron-beam lithography (EBL) [62, 63], focused ion beam lithography (FIB) [64-66], nanosphere lithography (NSL) [67, 68], nanoimprint lithography (NIL) [69-71], in general are used to generate reproducible SERS substrate. The EBL technique is based on the principle that resist change their property upon expose to the electron beam. In this technique, the desired pattern to be fabricated, is printed on the resist through electron beam. Direct writing

ability of FIB technique enable it to generate nanostructured substrate with different geometries. This technique is based on direct sputtering or milling of deposited thin metal layer. Both the EBL and FIB techniques are time consuming and costly process. Further, designing of SERS substrate through these processes demand very sophisticated instruments and laboratory setup. NSL is a highly flexible, inexpensive nanofabrication approach with control over nanostructures shape and size [72]. A monolayer of nanospheres typically of polystyrene is self assembled on a plane substrate which acts as a deposition mask. Other techniques such as spin coating, dropcasting, Langmuir-Blodgett etc. [73, 74] are also used for nanosphere deposition. Upon deposition of metal film on the mask using physical vapor deposition technique etching out of nanospheres by sonication results triangular shaped metal nanostructures array in the interstitial sites. Again, by using NIL technique a homogeneously patterned large area SERS substrate can be produced [69-71]. A rigid mask with desired nanopattern is developed using EBL technique and the pattern is transferred to polymer coated substrate. Metal film is deposited on the patterned substrate for SERS response. Before going for metal deposition one can go through etching process to get the desired pattern followed by metal deposition. The NIL technique is simple and cost effective and substrate can be largely reproducible. Difficulties in transferring of metal film on to desired substrate and fabrication of high aspect ratio structure are the main disadvantages of this technique. The SERS substrates produced by different fabrication techniques and their applications are summarized in table 1.1.

Table 1.1: Summery of different SERS substrate developed by different techniques

Substrate type	**Developing method**	**Architecture**	**Material and base**	**Parameters**	**Remarks**
Roughen electrodes [55, 75-77]	Electrochemical roughen	nanoparticle, nanocube	Palladium (Pd), Copper (Cu), Silver (Ag), Aluminium (Al)	EF few hundreds to 10^5, Relative standered deviation (RSD)= 12 %	Detection of chemicals, toxins etc.

Nano colloide [78-88]	chemical reduction, seed mediated, polyol process etc.	nanocluster, nanorod, nanoparticle, nanocube, nanostar, nanoshell	Gold (Au), Ag	EF= 10^3 - 10^{14}, Intensity variation upto 35 %, Detection limit upto single molecule	Detection of chemicals, biomolecules, pesticides, toxin, tracking of targeted drug etc.
Lithographic base	EBL [63, 89-94]	circular, triangular and square shaped nanoparticle, nanocones, nanoprism, nanohole, nanodisk, nanogrid, bowtie, nanopillar etc.	Au and Ag nanostructure on silicon and quartz substrate	EF= 10^4 to 10^{11}, Signal intensity deviation 11.5 %	Used for detection of biomolecules, toxic chemicals, acids etc.
	FIB [64-66]	nanorod, hexagon, shield, pentagon and kite like nanostructure	Au and Ag on Si substrate	EF= $> 10^7$	chemical sensing, virus detection.
	NSL [95-99]	nanotriangle, nanocap, nanobowl, nanosphere, nanohole, nanodisk, nanopillar	Au and Ag on Si and quartz base	FE= 10^4 to 10^{12} RSD= $< 5\%$	chemical, biosensing

	NIL [100-108]	nanodisk, nanotriangle, nanovoid, nanodome, nanocone, nanopillar	Au, Al, Ag on PDMS, PET sheet, polycarbonate sheet, Si, quartz base.	EF= 10^3 to 10^8, RSD= 9% and more,	biodetection, chemical detection, pesticides detection.
Biosilica [109-111]	Self-assembles, Inject printing	nanoparticle	Au, Ag on diatom frustule	Concentration as low as 10 pg/mL	biosensing, explosive chemical detection.
Rose petal [112, 113]	dropcast, physical vapor deposition	nanoparticle, nanolayer	Ag	EF=10^9, RSD=< 6 %, concentration as low as 10^{-13} M	Chemical detection.
DVD [114-116]	coating, electrochemical deposition, sputtering	particle, wire	Al, Au, Ag	EF= 10^4 to 10^6, RSD= 12-17%	acid and chemical detection
Paper [117-119]	evaporation, dipped in solution, dropcasting	nanorod, nanostar, nanoparticle etc.	Ag, Au	EF= 10^7 RSD= 6.19 %, as low as 0.6nM	Pesticides detection, chemical sensing, biomolecule sensing.

Other	nanostructure immobilizing on solid support by some means like self assembled, dropcast, PVD, dipped etc. [51, 120-122]	nanorod, nanoisland, nanowire, nanoparticle, nanocube, nanostar	Au, Ag	EF=10^9 LOD= 0.3 mg/L	Chemical sensing, food containment, Pesticides.
	AAO template for transferring nanostructure on to solid support [123-128]	nanocrater, nanoparticle, nanorod etc.	Au, Ag on Si, Cu	EF=10^9 RSD=< 5%, concentration as low as 10^{-14}	Pesticides, toxin in food, biomolecules.

Recent years have witnessed extensive research work related to development of SERS substrates by some new techniques and subsequently demonstrated the designed SERS substrate for different applications. Zhong et.al [129] prepared a self assembled Au and Ag core shell nanocube on polyvinyl chloride (PVC) base for onsite water pollutant monitoring. The group has synthesized Au and Ag core shell nanocube and immobilized them on PVC template and finally a thin film of Au was coated by dipping the nanocube immobilized PVC template into $HAuCL_4$ solution. With the designed SERS substrate, detection of thiram concentration as low as 0.1 ppb was reported. Fouad K et.al [130] developed a SERS substrate through attaching Au nanorod on Au coated Si substrate. The Au nanorods were immobilized on Au coated Si substrate by incubating the nanocolloid dispensed substrate for 5 days. The substrate has been used for detection of carbaryl in orange juice, grape juice and milk. Seungyoung Park et.al [131] developed a flexible SERS substrate by embedding gold nanostar in polydimethylsiloxane (PDMS) film. The synthesized gold nanostars were dip-coated on poly(diallyl dimethylammonium) (PDDA)coated Si substrate. The PDMS was poured on gold nanostars assembled Si sub-

strate and allowed to cure. Then, the cured PDMS was pilled off from the Si substrate. The substrate yields an enhancement factor of 1.9×10^8 while measuring Raman signal intensity from benzenethiol. Porous alloyed Au-Ag nanosphere array has been demonstrated as reproducible SERS substrate by Tao Zhang et.al [132]. Initially polystyrene microspheres were self assembled on Si substrate. Then an Au layer was coated by sputtering followed by annealing at certain temperature. The annealed substrate was then coated with Ag film and annealed again resulting in alloy of Au-Ag nanosphere SERS substrate. The substrate yields a good degree of reproducibility with RSD value 7.7% and EF of 4.37×10^7. Dip-coating triangular silver nanoplates onto cotton fiber have also been demonstrated as SERS substrate [133]. The usability of the substrate has been demonstrated for detection of pesticides. With this substrate 10 mM p-aminothiophenol has been detected with a maximum RSD value of 17%. In another work Kim et.al [107] have demonstrated Ag nanoparticle coated polyurethane acrylate nanopillar as SERS substrate. The polyurethane acrylate nanopillars were fabricated by etching through AAO template and Ag nanoparticles were attached by dipping it into the synthesized Ag colloidal solution. The substrate yields a maximum EF of 2.8×10^6 and RSD value of 9%. Binbin Jin et.al [134] have demonstrate Ag deposited lotus seedpod like structure as SERS substrate for detection of Alzheimers disease at its curable stage. The substrate was fabricated using NSL technique and it yields RSD from 4.1% to 8%. Naturally available micro/nanostructures have also been exploited for development of SERS substrate in recent years. Sharma et.al [106] have demonstrated the development of SERS substrate by transferring microstructure of plant leaf using soft lithography technique. Small pieces of leaf sample were fixed on glass and then polyvinylsiloxane (PVS) was dispensed on it followed by application of acute pressure. Upon curing, the mold was pilled off, resulting a negative template. The negative template was replicated to obtain positive structure. Synthesized Au nanoparticles were dropcasted onto the positive structure and dried to obtain the desired SERS substrate. With this substrate two herbicides were detected at nanomolar concentration level. Detection of methylene blue concentration as low as 0.1nM with RSD value of 10.4% has been demonstrated using that technique.

1.6 Scope of the thesis and statement of the thesis problem

The field of SERS has drawn significant interest towards its applicability in different fields of study. Obtaining a SERS substrate with good degree of reproducibility, longer

durability and high EF at an affordable cost is has been a long standing goal among researchers. This thesis work emphasize on obtaining of SERS substrate by adopting different low-cost approaches. It is needless to state that extensive research works are currently going on across the globe to obtain SERS substrates with different low-cost approaches. Most of the reported works do not meet all the features of SERS characteristics. For instance, the electrochemically roughen electrodes SERS substrates can be obtained at an affordable cost but it suffers from poor EF and reproducibility. Colloidal nanostructures can produce high EF but it yields low reproducibility. Though highly reproducible SERS substrates can be developed by using lithographic techniques, these techniques demand professional trainer for sample preparation and equipment operation, expensive, sophisticated instruments and laboratory facility, which eventually makes these substrates costly leading to limitation in its popularity. In this thesis work, an effort has been made to obtain SERS substrates through some inexpensive methods. The main idea is to design SERS substrates with high EF, better sensitivity, good degree of reproducibility by using minimum resources and instruments possible, that could emerge as a potential alternative to other sophisticated techniques. The first phase of this thesis work is focused on simulation of different metal nanostructures that generate strong LSPR field and using simulation tool. The optimized structure has been fabricated using EBL technique and the performance of the generated substrate has been evaluated by measuring Raman signal intensities for a Raman active sample. As this process is time consuming and expensive, in the next phase, low-cost techniques to obtain SERS substrate have been proposed. These techniques include obtaining of SERS substrates from diatom and printing grade papers. Au nanoparticles are incorporated in the surface and pores of the diatom frustule to obtain the SERS substrates. Similarly, by incorporating Ag nanoparticles in the micropores of printing grade paper SERS substrates have been obtained. These substrates have been initially characterized by measuring Raman signals from Raman active samples and its usability has been realized by detecting and quantifying fluoride level concentration in drinking water, glucose and artificial urine. These substrates yield good degree of Raman signal enhancement and reproducibility. In the third part, using gold coated electrospun polyvinylalcohol (PVA) nanofibers, low-cost SERS substrates with an acceptable reproducibility and relatively longer durability have been developed. After reliable characterization of the designed substrate using malachite green sample, the substrate has been used for detection of harmful pesticides commonly used in agriculture. In the final part of the thesis work, nano channels of blu-ray DVD (BRDVD) has been exploited for development of SERS substrate. Au nanoparticles are incorporated on BRDVD substrate and used for detection and quantification of three clinically important parameters in urine sample. This substrate yields high EF, good

degree of reproducibility and longer durability which can be obtained at an affordable cost.

References

[1] Primera-Pedrozo, O. M., Jerez-Rozo, J. I., De La Cruz-Montoya, E., Luna-Pineda, T., Pacheco-Londono, L. C., and Hernandez-Rivera, S. P. Nanotechnology-based detection of explosives and biological agents simulants. *IEEE Sensors Journal,* 8(6):963-973, 2008.

[2] Puppels, G., De Mul, F., Otto, C., Greve, J., Robert-Nicoud, M., Arndt-Jovin, D., and Jovin, T. Studying single living cells and chromosomes by confocal raman microspectroscopy. *Nature,* 347(6290):301, 1990.

[3] Peticolas, W., Patapoff T., Thomas, G., Postlewait, J., and Powell, J. Laser raman microscopy of chromosomes in living eukaryotic cells: Dna polymorphism in vivo. *Journal of Raman spectroscopy,* 27(8):571-578, 1996.

[4] Otto, C., De Grauw, C., Duindam, J., Sijtsema, N., and Greve, J. Applications of micro-raman imaging in biomedical research. *Journal of Raman spectroscopy,* 28(2-3):143-150, 1997.

[5] Cao, Y. C., Jin, R., and Mirkin, C. A. Nanoparticles with raman spectroscopic fingerprints for dna and rna detection. *Science,* 297(5586):1536-1540, 2002.

[6] Grubisha, D. S., Lipert, R. J., Park, H.-Y., Driskell, J., and Porter, M. D.Femtomolar detection of prostate-specific antigen: an immunoassay based on surface-enhanced raman scattering and immunogold labels. *Analytical chemistry,* 75(21):5936-5943, 2003.

[7] Jarvis, R. M. and Goodacre, R. Discrimination of bacteria using surface-enhanced raman spectroscopy. *Analytical chemistry,* 76(1):40-47, 2004.

[8] Eberhardt, K., Stiebing, C., Matthäus, C., Schmitt, M., and Popp, J. Advantages and limitations of raman spectroscopy for molecular diagnostics: an update. *Expert review of molecular diagnostics,* 15(6):773-787, 2015.

[9] Smith, E. and Dent, G. *Modern Raman spectroscopy: a practical approach.* John Wiley & Sons, 2013.

[10] Vankeirsbilck, T., Vercauteren, A., Baeyens, W., Van der Weken, G., Verpoort, F., Vergote, G., and Remon, J. P. Applications of raman spectroscopy in pharmaceutical analysis. *TrAC trends in analytical chemistry,* 21(12):869-877, 2002.

[11] Smekal, A. Zur quantentheorie der dispersion. *Naturwissenschaften,* 11(43):873-875, 1923.

[12] Raman, C. V. and Krishnan, K. S. A new type of secondary radiation. *Nature,* 121(3048):501, 1928.

[13] Theory of raman scattering. http://bwtek.com/raman-theory-of-raman-scattering.

[14] Fleischmann, M., Hendra, P. J., and McQuillan, A. J. Raman spectra of pyridine adsorbed at a silver electrode. *Chemical Physics Letters,* 26(2):163-166, 1974.

[15] Jeanmaire, D. L. and Van Duyne, R. P. Surface raman spectroelectrochemistry: Part i. heterocyclic, aromatic, and aliphatic amines adsorbed on the anodized silver electrode. *Journal of electroanalytical chemistry and interfacial electrochemistry,* 84(1):1-20, 1977.

[16] Albrecht, M. G. and Creighton, J. A. Anomalously intense raman spectra of pyridine at a silver electrode. *Journal of the american chemical society,* 99(15):5215-5217, 1977.

[17] Schatz, G., Young, M., and Van Duyne, R. *Surface enhanced raman scattering physics and applications,* 2006.

[18] Campion, A. and Kambhampati, P. Surface-enhanced raman scattering. *Chemical society reviews,* 27(4):241-250, 1998.

[19] Bhandari, D. *Surface-enhanced raman scattering: Substrate development and applications in analytical detection.* 2011.

[20] Brockman, J. M., Nelson, B. P., and Corn, R. M. Surface plasmon resonance imaging measurements of ultrathin organic films. *Annual review of physical chemistry,* 51(1):41-63, 2000.

[21] Knoll, W. Interfaces and thin films as seen by bound electromagnetic waves. *Annual Review of Physical Chemistry,* 49(1):569-638, 1998.

[22] Kelly, K. L., Coronado, E., Zhao, L. L., and Schatz, G. C. *The optical properties of metal nanoparticles: the influence of size, shape, and dielectric environment,* 2003.

[23] Haes, A. J., Haynes, C. L., McFarland, A. D., Schatz, G. C., Van Duyne, R. P., and Zou, S. Plasmonic materials for surface-enhanced sensing and spectroscopy. *MRS bulletin,* 30(5):368-375, 2005.

[24] Le Ru, E. and Etchegoin, P. *Principles of Surface-Enhanced Raman Spectroscopy: and related plasmonic effects.* Elsevier, 2008.

[25] Lombardi, J. R., Birke, R. L., Lu, T., and Xu, J. Charge-transfer theory of surface enhanced raman spectroscopy: Herzberg-teller contributions. *The Journal of chemical physics,* 84(8):4174-4180, 1986.

[26] Haynes, C. L. and Van Duyne, R. P. Plasmon-sampled surface-enhanced raman excitation spectroscopy. *The Journal of Physical Chemistry B,* 107(30):7426-7433, 2003.

[27] Bhandari, D., Wells, S. M., Retterer, S. T., and Sepaniak, M. J. Characterization and detection of uranyl ion sorption on silver surfaces using surface enhanced raman spectroscopy. *Analytical chemistry,* 81(19):8061-8067, 2009.

[28] Oran, J. M., Hinde, R. J., Abu Hatab, N., Retterer, S. T., and Sepaniak, M. J. Nanofabricated periodic arrays of silver elliptical discs as SERS substrates. *Journal of Raman Spectroscopy: An International Journal for Original Work in all Aspects of Raman Spectroscopy, Including Higher Order Processes, and also Brillouin and Rayleigh Scattering,* 39(12):1811-1820, 2008.

[29] Cho, W. J., Kim, Y., and Kim, J. K. Ultrahigh-density array of silver nanoclusters for SERS substrate with high sensitivity and excellent reproducibility. *ACS nano,* 6(1):249-255, 2011.

[30] Shanmukh, S., Jones, L., Driskell, J., Zhao, Y., Dluhy, R., and Tripp, R. A. Rapid and sensitive detection of respiratory virus molecular signatures using a silver nanorod array SERS substrate. *Nano letters,* 6(11):2630-2636, 2006.

[31] Olivares-Amaya, R., Rappoport, D., Munoz, P. A., Peng, P., Mazur, E., and Aspuru-Guzik, A. Can mixed-metal surfaces provide an additional enhancement to SERS? *The Journal of Physical Chemistry C,* 116(29):15568-15575, 2012.

[32] Aggarwal, R. L., Farrar, L. W., and Saikin, S. K. Increase of SERS signal upon heating or exposure to a high-intensity laser field: Benzenethiol on an agfon substrate. *The Journal of Physical Chemistry C,* 116(31):16656-16659, 2012.

[33] Banik, M., Nag, A., El-Khoury, P., Rodriguez Perez, A., Guarrotxena, N., Bazan, G., and Apkarian, V. Surface-enhanced raman scattering of a single nanodumbbell: dibenzyldithio-linked silver nanospheres. *The Journal of Physical Chemistry C,* 116(18):10415-10423, 2012.

[34] Pazos-Perez, N., Garcia de Abajo, F. J., Fery, A., and Alvarez-Puebla, R. A. From nano to micro: synthesis and optical properties of homogeneous spheroidal gold particles and their superlattices. *Langmuir,* 28(24):8909-8914, 2012.

[35] Fang, Y., Seong, N.-H., and Dlott, D. D. Measurement of the distribution of site enhancements in surface-enhanced raman scattering. *Science,* 321(5887):388-392, 2008.

[36] Liu, X., Sun, C.-H., Linn, N. C., Jiang, B., and Jiang, P. Wafer-scale surface enhanced raman scattering substrates with highly reproducible enhancement. *The Journal of Physical Chemistry C,* 113(33):14804-14811, 2009.

[37] Antoniou, E., Voudouris, P., Larsen, A., Loppinet, B., Vlassopoulos, D., Pastoriza-Santos, I., and Liz-Marzan, L. M. Static and dynamic plasmon-enhanced light scattering from dispersions of polymer-grafted silver nanoprisms in the bulk and near solid surfaces. *The Journal of Physical Chemistry C,* 116(6):3888-3896, 2012.

[38] Blaber, M. G., Henry, A.-I., Bingham, J. M., Schatz, G. C., and Van Duyne, R. P. Lspr imaging of silver triangular nanoprisms: correlating scattering with structure using electrodynamics for plasmon lifetime analysis. *The Journal of Physical Chemistry C,* 116(1):393-403, 2011.

[39] Correia-Ledo, D., Gibson, K. F., Dhawan, A., Couture, M., Vo-Dinh, T., Graham, D., and Masson, J.-F. Assessing the location of surface plasmons over nanotriangle and nanohole arrays of different size and periodicity. *The Journal of Physical Chemistry C,* 116(12):6884-6892, 2012.

[40] Tognalli, N. G., Fainstein, A., Calvo, E. J., Abdelsalam, M., and Bartlett, P. N. Incident wavelength resolved resonant SERS on Au sphere segment void (SSV) arrays. *The Journal of Physical Chemistry C,* 116(5):3414-3420, 2012.

[41] Steuwe, C., Kaminski, C. F., Baumberg, J. J., and Mahajan, S. Surface enhanced coherent anti-stokes raman scattering on nanostructured gold surfaces. *Nano letters,* 11(12):5339-5343, 2011.

[42] Liu, B. and Aydil, E. S. Growth of oriented single-crystalline rutile tio2 nanorods on transparent conducting substrates for dye-sensitized solar cells. *Journal of the American Chemical Society,* 131(11):3985-3990, 2009.

[43] Osberg, K. D., Rycenga, M., Harris, N., Schmucker, A. L., Langille, M. R., Schatz, G. C., and Mirkin, C. A. Dispersible gold nanorod dimers with sub-5 nm gaps as local amplifiers for surface-enhanced raman scattering. *Nano letters,* 12(7):3828-3832, 2012.

[44] Gabudean, A. M., Focsan, M., and Astilean, S. Gold nanorods performing as dualmodal nanoprobes via metal-enhanced fluorescence (mef) and surface-enhanced raman scattering (SERS). *The Journal of Physical Chemistry C,* 116(22):12240-12249, 2012.

[45] Liusman, C., Li, H., Lu, G., Wu, J., Boey, F., Li, S., and Zhang, H. Surface enhanced raman scattering of Ag-Au nanodisk heterodimers. *The Journal of Physical Chemistry C,* 116(18):10390-10395, 2012.

[46] Singh, J., Lanier, T. E., Zhu, H., Dennis, W. M., Tripp, R. A., and Zhao, Y. Highly sensitive and transparent surface enhanced raman scattering substrates made by active coldly condensed Ag nanorod arrays. *The Journal of Physical Chemistry C,* 116(38):20550-20557, 2012.

[47] Goh, M. S., Lee, Y. H., Pedireddy, S., Phang, I. Y., Tjiu, W. W., Tan, J. M. R., and Ling, X. Y. A chemical route to increase hot spots on silver nanowires for surface-enhanced raman spectroscopy application. *Langmuir,* 28(40):14441-14449, 2012.

[48] Zhang, L., Gong, X., Bao, Y., Zhao, Y., Xi, M., Jiang, C., and Fong, H. Electrospun nanofibrous membranes surface-decorated with silver nanoparticles as flexible and active/sensitive substrates for surface-enhanced raman scattering. *Langmuir,* 28(40):14433-14440, 2012.

[49] Tian, C., Ding, C., Liu, S., Yang, S., Song, X., Ding, B., Li, Z., and Fang, J. Nanoparticle attachment on silver corrugated-wire nanoantenna for large increases of surface-enhanced raman scattering. *Acs Nano,* 5(12):9442-9449, 2011.

[50] Yao, J.-L., Tang, J., Wu, D.-Y., Sun, D.-M., Xue, K.-H., Ren, B., Mao, B.-W., and Tian, Z.-Q. Surface enhanced raman scattering from transition metal nano-wire array and the theoretical consideration. *Surface science,* 514(1-3):108-116, 2002.

[51] Tao, A., Kim, F., Hess, C., Goldberger, J., He, R., Sun, Y., Xia, Y., and Yang, P. Langmuir- blodgett silver nanowire monolayers for molecular sensing using surfaceenhanced raman spectroscopy. *Nano letters,* 3(9):1229-1233, 2003.

[52] Mubeen, S., Zhang, S., Kim, N., Lee, S., Kramer, S., Xu, H., and Moskovits, M. Plasmonic properties of gold nanoparticles separated from a gold mirror by an ultrathin oxide. *Nano letters,* 12(4):2088-2094, 2012.

[53] Lin, X.-M., Cui, Y., Xu, Y.-H., Ren, B., and Tian, Z.-Q. Surface-enhanced raman spectroscopy: substrate-related issues. *Analytical and bioanalytical chemistry,* 394(7):1729-1745, 2009.

[54] Vo-Dinh, T. *Biomedical photonics handbook: biomedical diagnostics.* CRC press, 2014.

[55] Sardari, B. and Özcan, M. Real-time and tunable substrate for surface enhanced raman spectroscopy by synthesis of copper oxide nanoparticles via electrolysis. *Scientific reports,* 7(1):7730, 2017.

[56] Fan, M., Andrade, G. F., and Brolo, A. G. A review on the fabrication of substrates for surface enhanced raman spectroscopy and their applications in analytical chemistry. *Analytica chimica acta,* 693(1-2):7-25, 2011.

[57] Kneipp, K., Kneipp, H., Manoharan, R., Hanlon, E. B., Itzkan, I., Dasari, R. R., and Feld, M. S. Extremely large enhancement factors in surface-enhanced raman scattering for molecules on colloidal gold clusters. *Applied spectroscopy,* 52(12):1493-1497, 1998.

[58] Jena, B. K. and Raj, C. R. Seedless, surfactantless room temperature synthesis of single crystalline fluorescent gold nanoflowers with pronounced SERS and electrocatalytic activity. *Chemistry of Materials,* 20(11):3546-3548, 2008.

[59] Seo, D., Park, J. C., and Song, H. Polyhedral gold nanocrystals with o h symmetry: From octahedra to cubes. *Journal of the American Chemical Society,* 128(46):14863-14870, 2006.

[60] Tang, X.-L., Jiang, P., Ge, G.-L., Tsuji, M., Xie, S.-S., and Guo, Y.-J. Poly (n-vinyl-2-pyrrolidone)(pvp)-capped dendritic gold nanoparticles by a one-step hydrothermal route and their high SERS effect. *Langmuir,* 24(5):1763-1768, 2008.

[61] Maneerung, T., Tokura, S., and Rujiravanit, R. Impregnation of silver nanoparticles into bacterial cellulose for antimicrobial wound dressing. *Carbohydrate polymers,* 72(1):43-51, 2008.

[62] Fang, J., Du, S., Lebedkin, S., Li, Z., Kruk, R., Kappes, M., and Hahn, H. Gold mesostructures with tailored surface topography and their self-assembly arrays for surface-enhanced raman spectroscopy. *Nano letters,* 10(12):5006-5013, 2010.

[63] Yu, Q., Guan, P., Qin, D., Golden, G., andWallace, P. M. Inverted size-dependence of surface-enhanced raman scattering on gold nanohole and nanodisk arrays. *Nano letters,* 8(7):1923-1928, 2008.

[64] Lin, Y.-Y., Liao, J.-D., Ju, Y.-H., Chang, C.-W., and Shiau, A.-L. Focused ion beam-fabricated Au micro/nanostructures used as a surface enhanced raman scattering-active substrate for trace detection of molecules and in uenza virus. *Nanotechnology,* 22(18):185308, 2011.

[65] Sivashanmugan, K., Liao, J.-D., and Yao, C.-K. Nanovoids embedded in fib fabricated Au/Ag nanorod arrays for ultra sensitive SERS-active substrate. *Applied Physics Express,* 7(9):092202, 2014.

[66] Sivashanmugan, K., Liao, J.-D., You, J.-W., and Wu, C.-L. Focused-ion-beam fabricated Au/Ag multilayered nanorod array as SERS-active substrate for virus strain detection. *Sensors and Actuators B: Chemical,* 181:361-367, 2013.

[67] Yang, S., Xu, F., Ostendorp, S., Wilde, G., Zhao, H., and Lei, Y. Template-confined dewetting process to surface nanopatterns: Fabrication, structural tunability, and structure-related properties. *Advanced Functional Materials,* 21(13):2446-2455, 2011.

[68] Hulteen, J. C., Treichel, D. A., Smith, M. T., Duval, M. L., Jensen, T. R., and Van Duyne, R. P. Nanosphere lithography: size-tunable silver nanoparticle and surface cluster arrays. *The Journal of Physical Chemistry B,* 103(19):3854-3863, 1999.

[69] Alvarez-Puebla, R., Cui, B., Bravo-Vasquez, J.-P., Veres, T., and Fenniri, H. Nanoimprinted SERS-active substrates with tunable surface plasmon resonances. *The Journal of Physical Chemistry C,* 111(18):6720-6723, 2007.

[70] Lee, S.-W., Lee, K.-S., Ahn, J., Lee, J.-J., Kim, M.-G., and Shin, Y.-B. Highly sensitive biosensing using arrays of plasmonic Au nanodisks realized by nanoimprint lithography. *ACS nano,* 5(2):897-904, 2011.

[71] Kooy, N., Mohamed, K., Pin, L. T., and Guan, O. S. A review of roll-to-roll nanoimprint lithography. *Nanoscale research letters,* 9(1):320, 2014.

[72] Colson, P., Henrist, C., and Cloots, R. Nanosphere lithography: a powerful method for the controlled manufacturing of nanomaterials. *Journal of Nano- materials,* 2013:21, 2013.

[73] Liu, J., Chen, C., Yang, G., Chen, Y., and Yang, C.-F. Effect of the fabrication parameters of the nanosphere lithography method on the properties of the deposited Au-Ag nanoparticle arrays. *Materials,* 10(4):381, 2017.

[74] Ormonde, A. D., Hicks, E. C., Castillo, J., and Van Duyne, R. P. Nanosphere lithography: Fabrication of large-area Ag nanoparticle arrays by convective selfassembly and their characterization by scanning uv- visible extinction spectroscopy. *Langmuir,* 20(16):6927-6931, 2004.

[75] Liu, Z., Yang, Z.-L., Cui, L., Ren, B., and Tian, Z.-Q. Electrochemically roughened palladium electrodes for surface-enhanced raman spectroscopy: Methodology, mechanism, and application. *The Journal of Physical Chemistry C,* 111(4):1770-1775, 2007.

[76] Barber, T. E., List, M. S., Haas, J. W., and Wachter, E. A. Determination of nicotine by surface-enhanced raman scattering (SERS). *Applied spectroscopy,* 48(11):1423-1427, 1994.

[77] Ren, B., Lin, X.-f., Yan, J.-w., Mao, B.-w., and Tian, Z.-q. Electrochemically roughened rhodium electrode as a substrate for surface-enhanced raman spectroscopy. *The Journal of Physical Chemistry B,* 107(4):899-902, 2003.

[78] Zhang, W., Liu, J., Niu, W., Yan, H., Lu, X., and Liu, B. Tip-selective growth of silver on gold nanostars for surface-enhanced raman scattering. *ACS applied materials & interfaces,* 10(17):14850-14856, 2018.

[79] Deng, R., Qu, H., Liang, L., Zhang, J., Zhang, B., Huang, D., Xu, S., Liang, C., and Xu, W. Tracing the therapeutic process of targeted aptamer/drug conjugate on cancer cells by surface-enhanced raman scattering spectroscopy. *Analytical chemistry,* 89(5):2844-2851, 2017.

[80] Fazio, B., DAndrea, C., Foti, A., Messina, E., Irrera, A., Donato, M. G., Villari, V., Micali, N., Maragò, O. M., and Gucciardi, P. G. SERS detection of biomolecules at physiological ph via aggregation of gold nanorods mediated by optical forces and plasmonic heating. *Scientific reports,* 6:26952, 2016.

[81] Jorgenson, E. and Ianoul, A. Biofunctionalization of plasmonic nanoparticles with short peptides monitored by SERS. *The Journal of Physical Chemistry B,* 121(5):967-974, 2017.

[82] Matteini, P., Cottat, M., Tavanti, F., Panfilova, E., Scuderi, M., Nicotra, G., Menziani, M. C., Khlebtsov, N., de Angelis, M., and Pini, R. Site-selective surface enhanced raman detection of proteins. *ACS nano,* 11(1):918-926, 2016.

[83] Guo, P., Sikdar, D., Huang, X., Si, K. J., Xiong, W., Gong, S., Yap, L. W., Premaratne, M., and Cheng, W. Plasmonic core-shell nanoparticles for SERS detection of the pesticide thiram: size-and shape-dependent raman enhancement. *Nanoscale,* 7(7):2862-2868, 2015.

[84] Khoury, C. G. and Vo-Dinh, T. Gold nanostars for surface-enhanced raman scattering: synthesis, characterization and optimization. *The Journal of Physical Chemistry C,* 112(48):18849-18859, 2008.

[85] Niu, W., Chua, Y. A. A., Zhang, W., Huang, H., and Lu, X. Highly symmetric gold nanostars: crystallographic control and surface-enhanced raman scattering property. *Journal of the American Chemical Society,* 137(33):10460-10463, 2015.

[86] Childs, A., Vinogradova, E., Ruiz-Zepeda, F., Velazquez-Salazar, J. J., and Jose-Yacaman, M. Biocompatible gold/silver nanostars for surface-enhanced raman scattering. *Journal of Raman spectroscopy,* 47(6):651-655, 2016.

[87] Yang, J.-K., Kang, H., Lee, H., Jo, A., Jeong, S., Jeon, S.-J., Kim, H.-I., Lee, H.-Y., Jeong, D. H., Kim, J.-H., et al. Single-step and rapid growth of silver nanoshells as SERS-active nanostructures for label-free detection of pesticides. *ACS applied materials & interfaces,* 6(15):12541-12549, 2014.

[88] Sanchez-Gaytan, B. L., Swanglap, P., Lamkin, T. J., Hickey, R. J., Fakhraai, Z., Link, S., and Park, S.-J. Spiky gold nanoshells: synthesis and enhanced scattering properties. *The Journal of Physical Chemistry C,* 116(18):10318-10324, 2012.

[89] Gunnarsson, L., Bjerneld, E., Xu, H., Petronis, S., Kasemo, B., and Käll, M. Interparticle coupling effects in nanofabricated substrates for surface-enhanced raman scattering. *Applied Physics Letters,* 78(6):802-804, 2001.

[90] Liu, Y.-J., Zhang, Z.-Y., Zhao, Q., and Zhao, Y.-P. Revisiting the separation dependent surface enhanced raman scattering. *Applied Physics Letters,* 93(17):173106, 2008.

[91] Cinel, N. A., Cakmakyapan, S., Butun, S., Ertas, G., and Ozbay, E. E-beam lithography designed substrates for surface enhanced raman spectroscopy. *Photonics and Nanostructures-Fundamentals and Applications,* 15:109-115, 2015.

[92] Petti, L., Capasso, R., Rippa, M., Pannico, M., La Manna, P., Peluso, G., Calarco, A., Bobeico, E., and Musto, P. A plasmonic nanostructure fabricated by electron beam lithography as a sensitive and highly homogeneous SERS substrate for biosensing applications. *Vibrational Spectroscopy,* 82:22-30, 2016.

[93] Wu, T. and Lin, Y.-W. Surface-enhanced raman scattering active gold nanoparticle/nanohole arrays fabricated through electron beam lithography. *Applied Surface Science,* 435:1143-1149, 2018.

[94] Yue, W.,Wang, Z., Yang, Y., Chen, L., Syed, A.,Wong, K., andWang, X. Electron-beam lithography of gold nanostructures for surface-enhanced raman scattering. *Journal of Micromechanics and Microengineering,* 22(12):125007, 2012.

[95] Zhao, X., Wen, J., Zhang, M., Wang, D., Wang, Y., Chen, L., Zhang, Y., Yang, J., and Du, Y. Design of hybrid nanostructural arrays to manipulate SERS-active substrates by nanosphere lithography. *ACS applied materials & interfaces,* 9(8):7710-7716, 2017.

[96] Ho, C.-C., Zhao, K., and Lee, T.-Y. Quasi-3d gold nanoring cavity arrays with high-density hot-spots for SERS applications via nanosphere lithography. *Nanoscale,* 6(15):8606-8611, 2014.

[97] Hou, X., Wang, Q., Mao, G., Liu, H., Yu, R., and Ren, X. Periodic silver nanocluster arrays over large-area silica nanosphere template as highly sensitive SERS substrate. *Applied Surface Science,* 437:92-97, 2018.

[98] Im, H., Bantz, K. C., Lee, S. H., Johnson, T. W., Haynes, C. L., and Oh, S.-H. Selfassembled plasmonic nanoring cavity arrays for SERS and LSPR biosensing. *Advanced Materials,* 25(19):2678-2685, 2013.

[99] Wuytens, P. C., Skirtach, A. G., and Baets, R. On-chip surface-enhanced raman spectroscopy using nanosphere-lithography patterned antennas on silicon nitride waveguides. *Optics Express,* 25(11):12926-12934, 2017.

[100] Liu, G. L. and Lee, L. P. Nanowell surface enhanced raman scattering arrays fabricated by soft-lithography for label-free biomolecular detections in integrated microfluidics. *Applied Physics Letters,* 87(7):074101, 2005.

[101] Abu Hatab, N. A., Oran, J. M., and Sepaniak, M. J. Surface-enhanced raman spectroscopy substrates created via electron beam lithography and nanotransfer printing. *ACS nano,* 2(2):377-385, 2008.

[102] Ding, T., Sigle, D. O., Herrmann, L. O., Wolverson, D., and Baumberg, J. J. Nanoimprint lithography of Al nanovoids for deep-UV SERS. *ACS applied materials & interfaces,* 6(20):17358-17363, 2014.

[103] Krishnamoorthy, S., Krishnan, S., Thoniyot, P., and Low, H. Y. Inherently reproducible fabrication of plasmonic nanoparticle arrays for SERS by combining nanoimprint and copolymer lithography. *ACS applied materials & interfaces,* 3(4):1033-1040, 2011.

[104] Choi, C. J., Xu, Z.,Wu, H.-Y., Liu, G. L., and Cunningham, B. T. Surface-enhanced raman nanodomes. *Nanotechnology,* 21(41):415301, 2010.

[105] Suresh, V., Ding, L., Chew, A. B., and Yap, F. L. Fabrication of large-area flexible SERS substrates by nanoimprint lithography. *ACS Applied Nano Materials,* 1(2):886-893, 2018.

[106] Sharma, V. and Krishnan, V. Fabrication of highly sensitive biomimetic SERS substrates for detection of herbicides in trace concentration. *Sensors and Actuators B: Chemical,* 262:710-719, 2018.

[107] Kim, A. N., Lim, H., Lee, H. N., Park, Y. M., Yoo, B., and Kim, H.-J. Large-area and cost-effective fabrication of Ag-coated polymeric nanopillar array for surface enhanced raman spectroscopy. *Applied Surface Science,* 446:114-121, 2018.

[108] Wu, W., Hu, M., Ou, F. S., Li, Z., and Williams, R. S. Cones fabricated by 3d nanoimprint lithography for highly sensitive surface enhanced raman spectroscopy. *Nanotechnology,* 21(25):255502, 2010.

[109] Yang, J., Zhen, L., Ren, F., Campbell, J., Rorrer, G. L., and Wang, A. X. Ultrasensitive immunoassay biosensors using hybrid plasmonic-biosilica nanostructured materials. *Journal of biophotonics,* 8(8):659-667, 2015.

[110] Ren, F., Campbell, J., Rorrer, G. L., and Wang, A. X. Surface-enhanced raman spectroscopy sensors from nanobiosilica with self-assembled plasmonic nanoparticles. *IEEE Journal of Selected Topics in Quantum Electronics,* 20(3):127-132, 2014.

[111] Kong, X., Xi, Y., Le Duff, P., Chong, X., Li, E., Ren, F., Rorrer, G. L., and Wang, A. X. Detecting explosive molecules from nanoliter solution: A new paradigm of

SERS sensing on hydrophilic photonic crystal biosilica. *Biosensors and Bioelectronics,* 88:63-70, 2017.

[112] Chou, S.-Y., Yu, C.-C., Yen, Y.-T., Lin, K.-T., Chen, H.-L., and Su, W.-F. Romantic story or raman scattering? rose petals as ecofriendly, low-cost substrates for ultrasensitive surface-enhanced raman scattering. *Analytical chemistry,* 87(12):6017-6024, 2015.

[113] Xu, B.-B., Zhang, Y.-L., Zhang, W.-Y., Liu, X.-Q., Wang, J.-N., Zhang, X.-L., Zhang, D.-D., Jiang, H.-B., Zhang, R., and Sun, H.-B. Silver-coated rose petal: green, facile, low-cost and sustainable fabrication of a SERS substrate with unique superhydrophobicity and high efficiency. *Advanced Optical Materials,* 1(1):56-60, 2013.

[114] Dou, X., Chung, P.-Y., Jiang, P., and Dai, J. Surface plasmon resonance and surface-enhanced raman scattering sensing enabled by digital versatile discs. *Applied Physics Letters,* 100(4):041116, 2012.

[115] Giallongo, G., Pilot, R., Durante, C., Rizzi, G. A., Signorini, R., Bozio, R., Gennaro, A., and Granozzi, G. Silver nanoparticle arrays on a DVD-derived template: an easy & cheap SERS substrate. *Plasmonics,* 6(4):725, 2011.

[116] Leordean, C., Marta, B., Gabudean, A.-M., Focsan, M., Botiz, I., and Astilean, S. Fabrication of highly active and cost effective SERS plasmonic substrates by electrophoretic deposition of gold nanoparticles on a DVD template. *Applied Surface Science,* 349:190-195, 2015.

[117] Lee, M., Oh, K., Choi, H.-K., Lee, S. G., Youn, H. J., Lee, H. L., and Jeong, D. H. Subnanomolar sensitivity of filter paper-based SERS sensor for pesticide detection by hydrophobicity change of paper surface. *ACS sensors,* 3(1):151-159, 2018.

[118] Araújo, A., Pimentel, A., Oliveira, M. J., Mendes, M. J., Franco, R., Fortunato, E., Águas, H., and Martins, R. Direct growth of plasmonic nanorod forests on paper substrates for low-cost flexible 3D SERS platforms. *Flexible and Printed Electronics,* 2(1):014001, 2017.

[119] He, S., Chua, J., Tan, E. K. M., and Kah, J. C. Y. Optimizing the SERS enhancement of a facile gold nanostar immobilized paper-based SERS substrate. *RSC Advances,* 7(27):16264-16272, 2017.

[120] Su, Q., Ma, X., Dong, J., Jiang, C., and Qian, W. A reproducible SERS substrate based on electrostatically assisted aptes-functionalized surface-assembly of gold nanostars. *ACS applied materials & interfaces,* 3(6):1873-1879, 2011.

[121] Indrasekara, A. D. S., Meyers, S., Shubeita, S., Feldman, L., Gustafsson, T., and Fabris, L. Gold nanostar substrates for SERS-based chemical sensing in the femtomolar regime. *Nanoscale,* 6(15):8891-8899, 2014.

[122] Han, C., Yao, Y., Wang, W., Qu, L., Bradley, L., Sun, S., and Zhao, Y. Rapid and sensitive detection of sodium saccharin in soft drinks by silver nanorod array SERS substrates. *Sensors and Actuators B: Chemical,* 251:272-279, 2017.

[123] Fu, Q., Zhan, Z., Dou, J., Zheng, X., Xu, R., Wu, M., and Lei, Y. Highly reproducible and sensitive SERS substrates with Ag inter-nanoparticle gaps of 5 nm fabricated by ultrathin aluminum mask technique. *ACS applied materials & interfaces,* 7(24):13322-13328, 2015.

[124] Celik, M., Altuntas, S., and Buyukserin, F. Fabrication of nanocrater-decorated anodic aluminum oxide membranes as substrates for reproducibly enhanced SERS signals. *Sensors and Actuators B: Chemical,* 255:2871-2877, 2018.

[125] Geng, F., Zhao, H., Fu, Q., Mi, Y., Miao, L., Li, W., Dong, Y., Wu, M., and Lei, Y. Gold nanochestnut arrays as ultra-sensitive SERS substrate for detecting trace pesticide residue. *Nanotechnology,* 29(29):295502, 2018.

[126] Huang, Z., Meng, G., Huang, Q., Chen, B., Zhu, C., and Zhang, Z. Large-area Ag nanorod array substrates for SERS: AAO template-assisted fabrication, functionalization, and application in detection pcbs. *Journal of Raman Spectroscopy,* 44(2):240-246, 2013.

[127] Yan, B., Sun, K., Chao, K., Alharbi, N. S., Li, J., and Huang, Q. Fabrication of a novel transparent SERS substrate comprised of Ag-nanoparticle arrays and its application in rapid detection of ractopamine on meat. *Food Analytical Methods,* 1-7, 2018.

[128] Lim, L., Ng, B., Fu, C., Tobing, L. Y., and Zhang, D. Highly sensitive and scalable AAO-based nano-fibre SERS substrate for sensing application. *Nanotechnology,* 28(23):235302, 2017.

[129] Zhong, L.-B., Liu, Q., Wu, P., Niu, Q.-F., Zhang, H., and Zheng, Y.-M. Facile on-site aqueous pollutant monitoring using a flexible, ultralight, and robust

surface-enhanced raman spectroscopy substrate: Interface self-assembly of Au Ag nanocubes on a polyvinyl chloride template. *Environmental Science & Technology,* 52(10):5812-5820, 2018.

[130] Alsammarraie, F. K. and Lin, M. Using standing gold nanorod arrays as surface enhanced raman spectroscopy (SERS) substrates for detection of carbaryl residues in fruit juice and milk. *Journal of agricultural and food chemistry,* 65(3):666-674, 2017.

[131] Park, S., Lee, J., and Ko, H. Transparent and flexible surface-enhanced raman scattering (SERS) sensors based on gold nanostar arrays embedded in silicon rubber film. *ACS applied materials & interfaces,* 9(50):44088-44095, 2017.

[132] Zhang, T., Sun, Y., Hang, L., Li, H., Liu, G., Zhang, X., Lyu, X., Cai, W., and Li, Y. Periodic porous alloyed Au-Ag nanosphere arrays and their highly sensitive SERS performance with good reproducibility and high density of hotspots. *ACS applied materials & interfaces,* 10(11):9792-9801, 2018.

[133] Cheng, D., He, M., Ran, J., Cai, G., Wu, J., and Wang, X. Depositing a flexible substrate of triangular silver nanoplates onto cotton fabrics for sensitive SERS detection. *Sensors and Actuators B: Chemical,* 270:508-517, 2018.

[134] Jin, B., He, J., Li, J., and Zhang, Y. Lotus seedpod inspired SERS substrates: A novel platform consisting of 3D sub-10 nm annular hot spots for ultrasensitive SERS detection. *Advanced Optical Materials,* 1800056, 2018.